frontiers | Frontiers in Earth Science

TYPE Original Research
PUBLISHED 19 July 2023
DOI 10.3389/feart.2023.1115235

OPEN ACCESS

EDITED BY
Hai Lin,
Nanchang University, China

REVIEWED BY
Asimina Athanatopoulou,
Aristotle University of Thessaloniki, Greece
Baki Ozturk,
Hacettepe University, Türkiye

*CORRESPONDENCE
Dewen Liu,
civil_liudewen@sina.com
Shunzhong Yao,
yaoswfu@163.com

SPECIALTY SECTION
This article was submitted to Geohazards and Georisks, a section of the journal Frontiers in Earth Science

RECEIVED 03 December 2022
ACCEPTED 01 February 2023
PUBLISHED 19 July 2023

CITATION
Shu T, Li H, Wang T, Liu D, Yao S and Lei M (2023), Study on the seismic response of new staggered story isolated structure under different parameters.
Front. Earth Sci. 11:1115235.
doi: 10.3389/feart.2023.1115235

Study on the seismic response of new staggered story isolated structure under different parameters

Tong Shu[1], Hong Li[1], Taize Wang[1], Dewen Liu[1]*, Shunzhong Yao[1]* and Min Lei[2]

[1]College of Civil Engineering, Southwest Forestry University, Kunming, Yunnan, China, [2]School of Civil Engineering, Southwest Jiaotong University, Chengdu, Sichuan, China

The new staggered story isolated structure is developed according to the base-isolated structure and the mid-story isolated structure. Quantitative calculation and evaluation of seismic damage are very important for structural safety. In this paper, the seismic damage evaluation of a new staggered story isolated structure is studied by numerical simulation and damage index calculation. A new staggered story isolated structure is established, and the effects of different layers and different chassis areas on the seismic response of the structure are studied. When the position of the bottom isolated layer stays the same, the upper isolated layer is set at different layers, which is set to the top of the 3rd, 6th and 9th layers. When the upper isolated layer keeps at the top of the 3rd layer, the chassis area is set at a different area, which is 26 m × 26 m, 36 m × 36 m and 46 m × 46 m. The results show that the new staggered story isolated structure has good isolated effects under the ground motion. For the structure set upper isolation layer is lower, the inter-layer shear force, inter-layer acceleration and inter-layer displacement are reduced. The energy dissipation effect of the structure improves. The core tube is less damaged and the plastic hinge is smaller. With the increase of chassis area, the isolated effect of the part above the upper isolated layer is good, while the shear force and acceleration of the part below the upper isolated layer of the structure increase, the damage at the core tube changed little and the appearance of the plastic hinge increased. Under earthquakes, with the change in position of the upper isolated layer and the area of the chassis of the new staggered story isolated structure, the displacement, tensile stress and compressive stress of the isolated bearing still meet the requirements of the standard.

KEYWORDS

new staggered story isolated building, shock absorption effect, time history analysis, seismic response, earthquake

1 Introduction

Base isolated structures and mid-isolated structures are the focus of research on disaster prevention and mitigation. Based on this, the new staggered story isolated structure structure has been developed. The isolated layer of the base isolated structure and the mid-story isolated structure is located on a specific structure layer. In comparison, the isolated layer of the new staggered mid-story isolated structure can be set on different layers of the structure

(Liu et al., 2022; Zhang Y F et al., 2022). The new staggered story isolated structure has been implemented in practical projects. For instance, after the Istanbul earthquake, a hospital was strengthened with a new staggered story isolated structure (Erdik et al., 2018).

Since earthquakes occur frequently around the world, the research on isolated structures has been more and more focused. The base-isolated structure can successfully protect buildings during powerful earthquakes (Losanno et al., 2021) and relieve the seismic response of structures (Cancellara and De Angelis, 2016); (Hayashi et al., 2018); (Park and Ok, 2021); (Pérez-Rocha et al., 2021); (Qahir Darwish and Bhandari, 2022). Fujii (2022) studied the influence of long-period pulse-type ground motion input angle of seismic incidence (ASI) on buildings with irregular base isolation and concluded that the ground motion spindle defined by cumulative energy input was more suitable for discussing the influence of ASI on the response of buildings with irregular base isolation (Micozzi et al., 2022). studied the seismic response and seismic risk of the base isolation structure in the RINTC project and concluded that the isolation structure can effectively limit the damage. According to the study (Wang et al., 2022), The semi-active tuned mass damper can effectively improve the displacement and acceleration performance of linear and non-linear base isolation structures (Vibhute et al., 2022). Research shows that both Friction Pendulum System (FPS) and Lead Rubber Bearing (LRB) isolation frames can effectively increase the seismic performance of structures (Zhao et al., 2022). Research shows that the pulse signal in pulsed ground motion will amplify the response of LRB base isolation structure (Nobari Azar et al., 2022). found that natural rubber base isolation can effectively meet the requirements of base isolation system (Rabiee and Chae, 2022). transmissibility-based semi-active (TSA) controller enables the system to have high damping under the action of long period ground motion and low damping under the action of short period ground motion, showing unique effects. The study shows the performance of linear shear layer structure with non-linear base isolation bearing. TMD can effectively change the performance of the isolation structure and increase the isolation effect (Hessabi et al., 2017; Ozturk et al., 2022). Köroğlu (2022) study found that the viscous damper can effectively increase the isolation effect of the structure. The method of machine learning has significance for the research of seismic isolated structure, and it has a high sensitivity rate prediction accuracy to put forward the early warning of disasters (Chang et al., 2022a; Chang et al., 2022b; Huang et al., 2022d).

The development of base isolation structures has been a long process, and it has been widely used all over the world. However, (Li et al., 2022), comprehensively investigated the seismic response of the simplified model and the story-separated seismic building, and the analysis showed that the simplified building model could provide accurate estimation of the important seismic response (Hur and Park, 2022). proposed a method to reduce the seismic load related to vertical strengthening of buildings while improving the seismic performance (Zhang S et al., 2022). proved that the damping coefficient of the Kelvin-Voigt model has a great influence on the mean square error of the total vibration energy, while the stiffness coefficient is less sensitive to it by comparing the seismic scheme and the layered interval seismic scheme (Ma et al., 2020). The dynamic response characteristics of the three structures under near-fault pulse-like ground motions are analysed and compared with the far-fault ground motions (Saha and Mishra, 2021a). found that storey interval earthquakes can effectively reduce the seismic vulnerability and loss of buildings under the action of ground motion, and increase the influence of resilience (Saha and Mishra, 2021b). Storey interval shock (ISI) shows good damping effect in relatively tall buildings (Donà et al., 2021). As shown in some studies, fluid viscous dampers (FVDs) installed in isolation systems can effectively reduce the deflections of isolators, but amplify the interstory displacement and floor acceleration (Li et al., 2014). This study found that both base isolation and layer interval shock have good isolation effect, and the isolation performance of base isolation structure is better than that of story-adding structure (Faiella et al., 2020). In this study, the model of story-separated seismic structure was established and it was found that the model effectively reduced the seismic response (Wu et al., 2019). This study will improve the understanding of eccentric structures with tower podium and provide guidance for the seismic design of such structures. Use machine learning methods to predict the occurrence of disasters in different environments (Huang et al., 2020a; Huang et al., 2020b; Huang et al., 2020c).

Theories are relatively complete for large chassis seismic structures (Pang., 2012; Li et al., 2021). The tower building on the large chassis is characterized by vertical irregularity. The isolated layer is set where the structure occurs an abrupt change by using the layer spacing technology to consume seismic energy and avoid the problem of complex internal force at the abrupt change of the stiffness (Zhang H et al., 2021). The seismic performance of the multi-tower foundation isolated structure is discussed, and the parameters such as inter-story displacement, shear force and displacement angle of the structure under ground motion are analyzed. The results show that the base-isolated structure has a favourable damping effect and can effectively suppress the structural torsion (Wang and Lei, 2021; Zhou, Y et al., 2018). Guo et al. (2021) improved the accuracy of the disaster prediction and used machine learning methods to predict and monitor the occurrence of disasters (Jiang et al., 2018).

According to the above analysis, most research currently focuses on the base-isolated structure and the mid-story isolated structure. However, there are fewer studies on the new staggered story isolated structure.

In this paper, the seismic response of a new staggered story isolated structure under ground motion is studied. The relationship between the upper and lower parts of the new staggered story isolated structure, the volume, the section of the component, the parameters of the isolation bearing and the layout principle are introduced. Under ground motions, the damping effect, structural damage, structural energy consumption, and the response of the isolated bearing of the innovative staggered story isolated structure are obtained. This research is expected to provide a reference for the design and development of the new staggered story isolated structure.

2 Methods and materials

2.1 Project overview

In order to verify the isolation effect of the new staggered story isolated structure under the action of ground motion, a

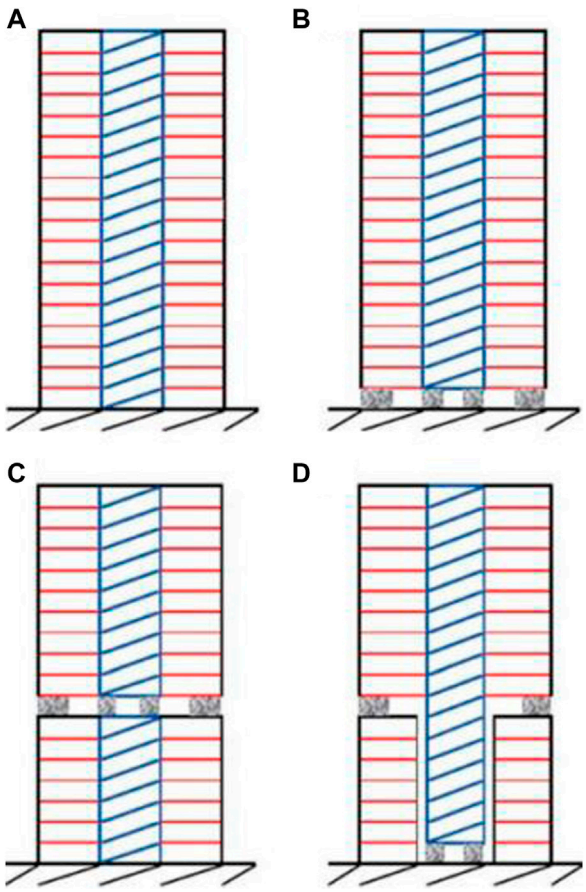

FIGURE 1
Structure diagram: **(A)** aseismic structure, **(B)** base-isolated structure, **(C)** mid-story isolated structure, **(D)** new staggered story isolated structure (The blue part represents the core tube, the red part represents the frame, and the shadow part represents the isolated bearings).

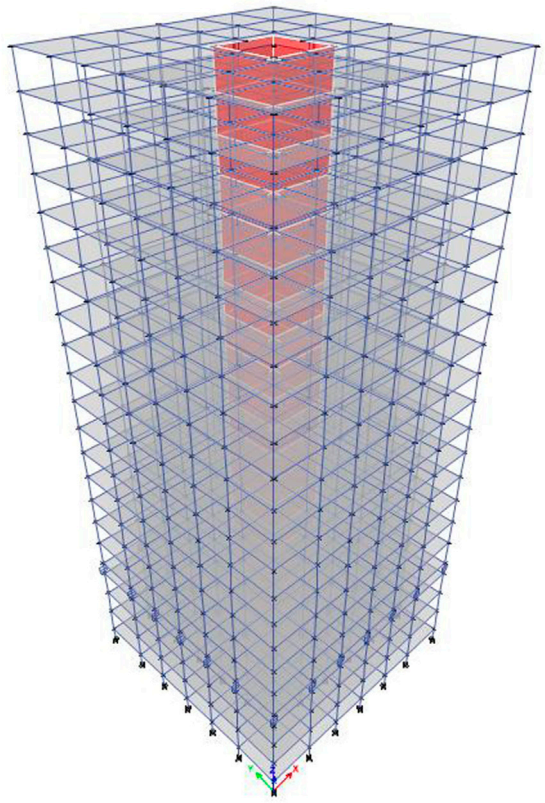

FIGURE 2
3D diagram of the new staggered story isolated structure.

frame-core tube structure with 20 layers, each layer is 4 m high and the building plane structure size is 26 m × 26 m is built. Figure 1 shows the aseismic structure, the base-isolated structure, the mid-story isolated structure, and the new staggered story isolated structure. Figure 2 depicts the three-dimensional finite element model of the structure. The seismic fortification grade is B, and the seismic fortification intensity is 8 (0.20 g) and the seismic group is designed to be Group II. The sectional dimensions of the structure can be seen in Table 1, Table 2. C40 concrete non-linear material was defined with Takeda hysteresis type and HRB400 steel reinforcement non-linear material was defined with Kinematic hysteresis type. The frame column is designated as PMM plastic hinge, and the frame beam and connecting beam are designated as M3 plastic hinge. The bottom two-layer core tube of the stratified separated seismic structure is the bottom strengthening area, which is adopted simulation of layered shell. The rest were non-bottom reinforced areas, which were simulated by elastic thin shell elements. The thickness of the concrete cover is 50 mm. The shear walls were simulated by thin shell elements with a concrete thickness of 250 mm.

2.2 Modelling

The ETABS software is used to extract the column bottom reaction f at the isolation support under the standard value of gravity load, and then the number and model of isolation supports are estimated according to the total horizontal yield force as 2% of the column bottom reaction under the standard value of gravity load. The isolation support LRB1000 is used for the core and LRB600 for the frame. The parameters of isolation bearings are shown in Table 2 below, and their arrangement is shown in Figure 3. Isolation bearing adopts Rubber Isolator and Gap elements to simulate the Vertical tension and compression non-linear stiffness. In order to make the restoring force characteristics of the isolation layer more consistent with the actual situation, Bouc-Wen model was used to represent the restoring force model of the isolation layer in the subsequent time history analysis.

2.3 Earthquake wave selection

The seismic fortification intensity is set to degree 8, and the basic acceleration of the earthquake is set to 0.2 g. Meanwhile, the site category is class 2, and the seismic group is designed as group III. The EMC wave, DUZCE wave and artificial wave are selected. Table 3 shows the information regarding the acceleration

TABLE 1 Frame section parameters.

Component type	Component location/Layer	Section size	
		Height/mm	Width/mm
Framed Column	1–20	800	800
Framed Column	1–20	700	350

TABLE 2 Shear wall section parameters.

Section type	Section Name	Element type	Thickness of concrete layer/mm
Shear Wall	Wall-250	Thin Shell	250

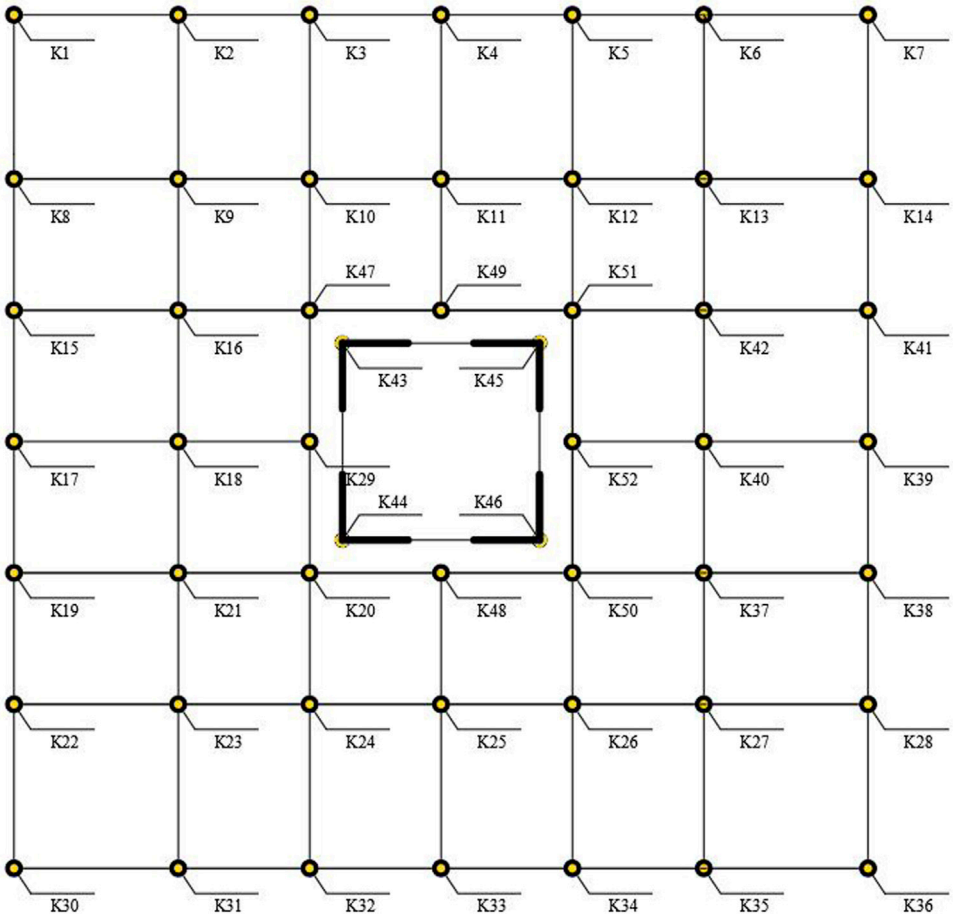

FIGURE 3
Layout of isolated bearings.

response spectrum of the ground motion. The acceleration response spectrum of the ground shaking is shown in Figure 4. When the input of three groups of acceleration time history curves is taken, the envelope values of the time history method and the larger values of the mode decomposition response spectrum method are appropriate for the calculation results. When using the time-history analysis method, the actual strong earthquake records and artificial simulated acceleration

TABLE 3 Parameters of isolated bearings.

Model	Effective diameter/mm	Total rubber thickness/mm	Total stiffness before yield/kN·m	Equivalent stiffness		Vertical stiffness/kN·mm	Yield force/kN
				100% horizontal shear deformation/kN·m	250% horizontal shear deformation/kN·m		
LRB600	600	112	16.39	1.83	1.83	2,200	63
LRB1000	1,000	186	27.08	3.19	3.19	4,300	203

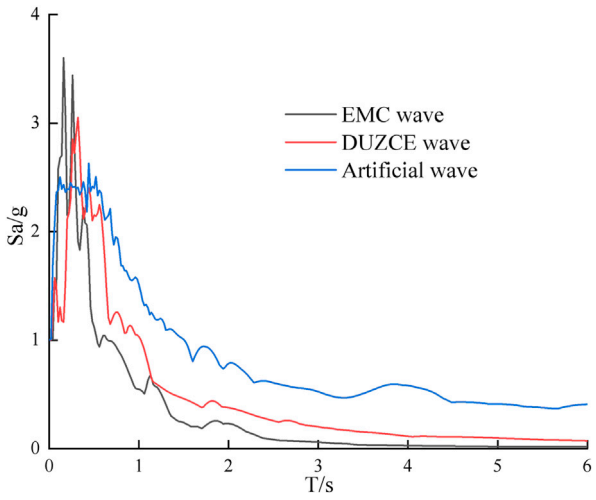

FIGURE 4
Acceleration response spectrum.

time-history curves should be selected according to the type of building site and the design earthquake group, among which the number of actual strong earthquake records should not be less than 2/3 of the total number. The average seismic influence coefficient curve of multiple groups of time-history curves should be statistically consistent with the seismic influence coefficient curve adopted by the mode decomposition response spectrum method. In elastic time history analysis, the base shear force calculated by each time history curve should not be less than 65% of the result calculated by mode decomposition response spectrum method, and the average value of the base shear force calculated by multiple time history curves should not be less than 80% of the result calculated by mode decomposition response spectrum method.

3 Analysis of the shock absorption effect

The main difference between the new staggered isolated structure, the base-isolated structure, and the mid-story isolated structure is that the shear displacement and acceleration of the core tube and frame of the latter two kinds of structures are consistent. However, for the new staggered isolated structure with two layers, the displacement and acceleration of the core tube and the frame above the third layer keep consistent, while the core tube and the frame below the lower isolated layer are separate, and their shear displacement and acceleration are different. By integrating and analyzing the acceleration time-history data at each time step, the dynamic response state of the structure at each time step is determined. The dynamic time history analysis is conducted under the earthquake motions (peak acceleration of 200 cm/s^2) to get the seismic response and the energy dissipation of a new staggered story isolated structure.

3.1 Seismic response analysis of a new staggered isolated structure with different fault heights

In order to compare and study the effect of different staggered layer heights on the new staggered layer isolated structure, the seismic structure model and three different new staggered story isolated structure models were established with the upper isolated layer set on the top of the 3rd floor (Model 1), the 6th floor (Model 2) and the 9th floor (Model 3), respectively, while keeping the large chassis area and the position of the isolated layer at the bottom of the core tube unchanged. The models are shown in Figure 5.

3.1.1 Modal period

Table 5 compares the results of the first three modal periods for the aseismic structure and the new staggered story isolated structure (when the upper isolated layer is set at the top of the 3rd floor, the 6th floor and the 9th floor). It can be seen from Table 4 that the period of the first three steps of the new staggered story isolated structure is greater than that of the aseismic structure. When the chassis area of the new staggered story isolated structure remains unchanged, the lower the upper isolated layer is, the smaller the modal period of the whole structure is.

3.1.2 Basal shear force

Figure 6 depicts the comparison of the base shear force between the aseismic structure and the new staggered story isolated structure with different positions of the staggered layer. It can be seen that compared with the aseismic structure, the base shear force of the new staggered story isolated structure (the upper isolated layer is set at the top of the 3rd floor, the 6th floor and the 9th floor) is reduced under the action of the ground motion, and the isolation effect is better. When the chassis area is the same, the lower the upper isolated

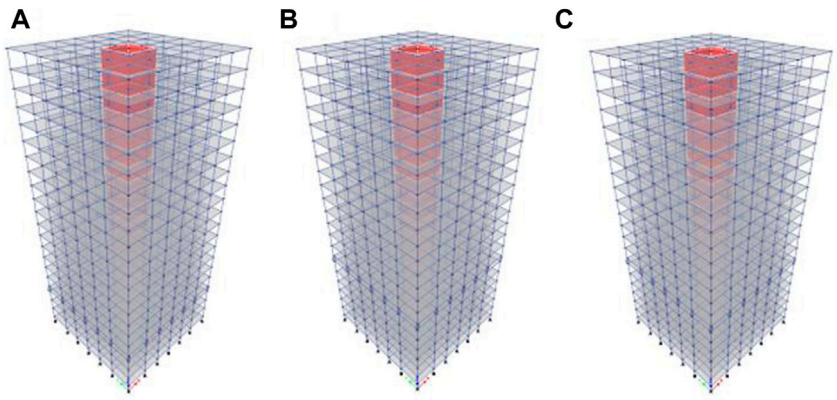

FIGURE 5
New staggered layer isolated structure with different isolated layers **(A)** Model 1, **(B)** Model 2, **(C)** Model 3.

TABLE 4 Basic information of earthquake motions.

Earthquake	Magnitude	Epicentral distance/km	PGA/cm s 2
EMC wave	6.9	25	42.8
DUZCE wave	6.9	65	145.8
Artificial wave	/	/	/

TABLE 5 The first three modal periods of the new staggered isolated structure with different fault heights.

Type of construction	First cycle	Second cycle	Third cycle
Aseismic structure	1.069	1.069	0.983
Model 1	2.712	2.712	2.645
Model 2	2.556	2.556	2.477
Model 3	2.37	2.37	2.275

layer is, the smaller the base shear force of the structure, and the better the isolated effect.

3.1.3 Inter-laminar shear force

The finite element models of the aseismic structure and the new staggered story isolated structure are developed. The dynamic time history analysis is conducted under the earthquake motions with the seismic fortification intensity of degree 8 (peak acceleration of 200 cm/s^2). Figure 7 depicts the comparison of the inter-laminar shear force between the aseismic structure and the new staggered story isolated structure (when the upper isolated layer is set at the top of the column of the 3rd floor, the 6th floor and the 9th floor). It can be seen that compared to the seismic structure, the new staggered story isolated structure has a certain damping effect; the inter-laminar shear force is sharply decreased, and that of the core tube below the upper

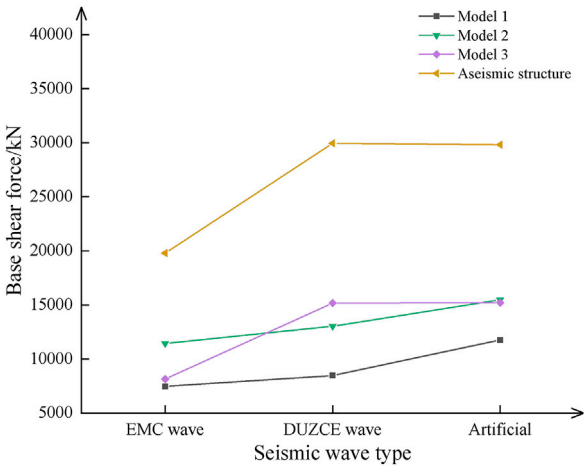

FIGURE 6
The comparison of the base shear force between the aseismic structure and the new staggered story isolated structure with different position of the isolated layer.

isolated layer of the new staggered story isolated structure is superior to the frame. The shear force of the part of the frame below the upper isolated layer is greater than that of the core tube. The isolated effect of the core tube part is better than that of the frame part, and the lower the upper isolated layer is, the better the isolated effect will be.

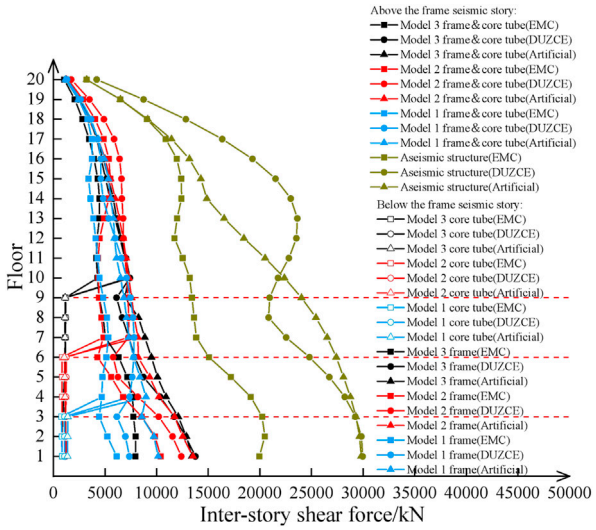

FIGURE 7
Story shear force.

3.1.4 Story displacement

Figure 8 illustrates the comparison of displacement between the aseismic structure and the new staggered story isolated structure (when the upper isolated layer is set at the top of the column of the 3rd floor, the 6th floor and the 9th floor). It can be seen that the displacement of the new staggered story isolated structure mainly occurs in the isolated layer. Compared to the seismic structure, there occurs some deformation in the upper structure of the new staggered story isolated structure, but it is greatly reduced. The average vertex displacement of the new staggered story isolated structure is slightly smaller than that of the non-isolated structure, and the part above the upper isolated layer is approximately flat. The displacement of the frame part below the upper isolated layer is greater than that of the core tube. The lower the upper isolated layer is, the smaller the displacement of the frame and the core tube is.

3.1.5 Inter-layer acceleration

The comparison of the inter-layer acceleration between the seismic structure and the new staggered story isolated structure (when the upper isolated layer is set at the top of the column of the 3rd floor, the 6th floor and the 9th floor) is shown in Figure 9. According to Figure 9, the acceleration of the new staggered story isolated structure above the upper isolated layer is reduced compared to the seismic structure. The inter-layer acceleration of the core tube below the upper isolated layer of the frame decreases while the inter-layer acceleration of the frame increases.

3.1.6 Structural energy consumption

The comparison of the energy dissipation between the seismic structure and the new staggered story isolated structure (when the upper isolated layer is set at the top of the column of the 3rd floor, the 6th floor and the 9th floor) is shown in Table 6. It can be seen from Table 6 That when the chassis area of the new staggered story isolated structure remains unchanged, the lower the upper isolated layer, the more favourable the effect of the energy dissipation, and therefore the better the isolated effect.

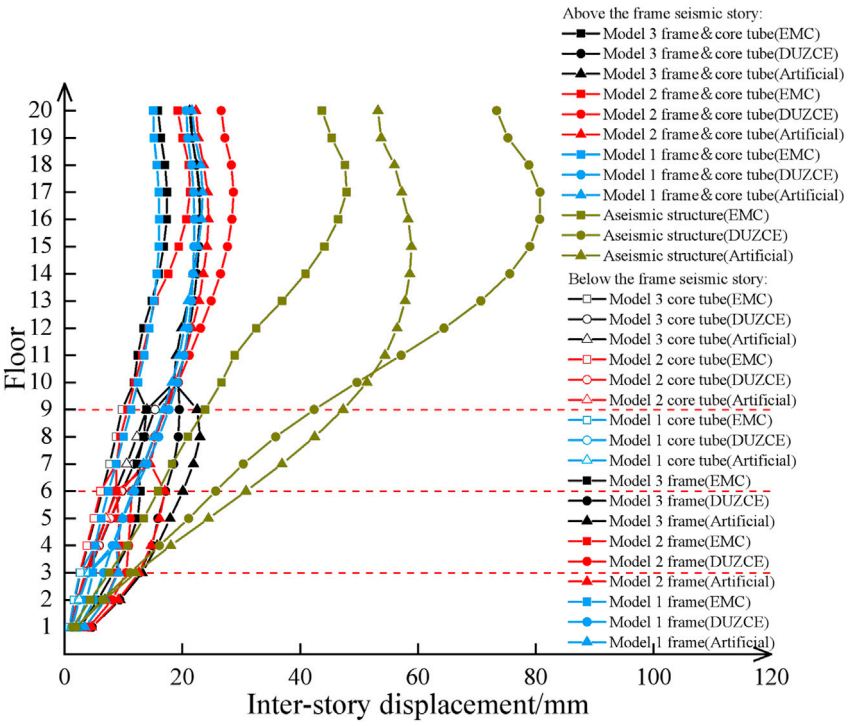

FIGURE 8
Story displacement.

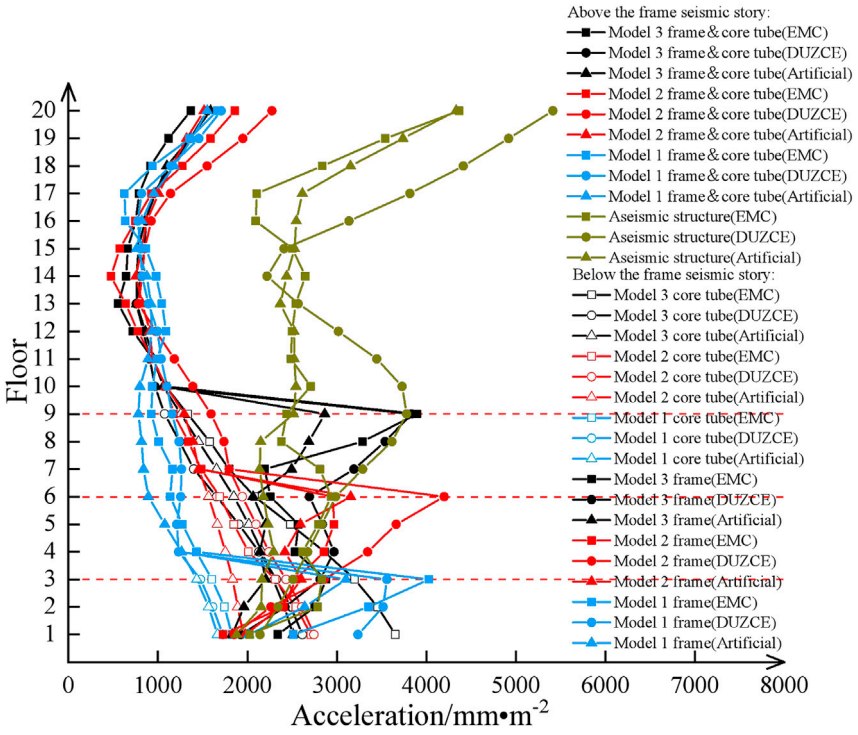

FIGURE 9
Story acceleration.

TABLE 6 Energy consumption of the new staggered story isolated structure.

Type of construction	Earthquake wave	Total seismic input energy (KN·m)	Self damping energy dissipation of structure (KN·m)	Energy consumption of isolated layer (KN·m)	Energy consumption rate of isolated layer (%)	Average decreasing amplitude ratio (%)
Model 1	EMC wave	2018.77	715.63	1,287.78	63.80	70.40
	DUZCE wave	1729.05	512.20	1,208.36	66.90	
	Artificial wave	5,470.61	1,235.08	4,234.36	77.40	
Model 2	EMC wave	2,867.63	1,203.07	1,646.93	57.40	65.50
	DUZCE wave	1942.21	659.22	1,273.74	65.60	
	Artificial wave	5,555.00	1,654.58	4,074.15	73.30	
Model 3	EMC wave	2,804.39	1,213.05	1,574.63	56.10	63.90
	DUZCE wave	2,286.71	805.16	1,471.12	64.30	
	Artificial wave	6,213.82	1780.01	4,429.13	71.30	

3.2 Seismic response analysis of the new staggered story isolated structure with different large chassis areas

In order to comparatively study the influence of different large chassis areas on the new staggered story isolated structure, the upper isolated layer was kept at the top of the third layer, and three different types of new staggered story isolated structures with large chassis areas of 26 m × 26 m (Model 1), 36 m × 36 m (Model 4) and 46 m × 46 m (Model 5) are comparatively analyzed, as shown in Figure 10.

3.2.1 Modal period

Table 7 compares the results of the first three modal periods for the new staggered story isolated structure with

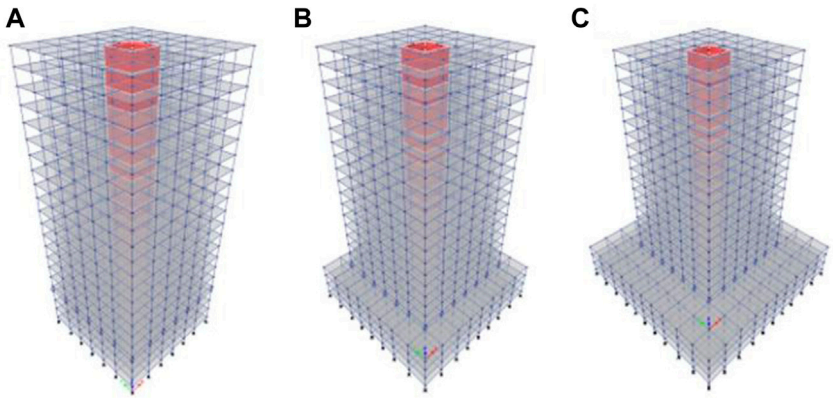

FIGURE 10
New staggered layer isolated structure with different chassis area **(A)** Model 1, **(B)** Model 4, **(C)** Model 5.

TABLE 7 The first three modal periods of the new staggered isolated structure with different chassis area.

Type of construction	First cycle	Second cycle	Third cycle
Aseismic structure	1.069	1.069	0.983
Model 1	2.712	2.712	2.645
Model 4	2.658	2.658	2.577
Model 5	2.645	2.645	2.567

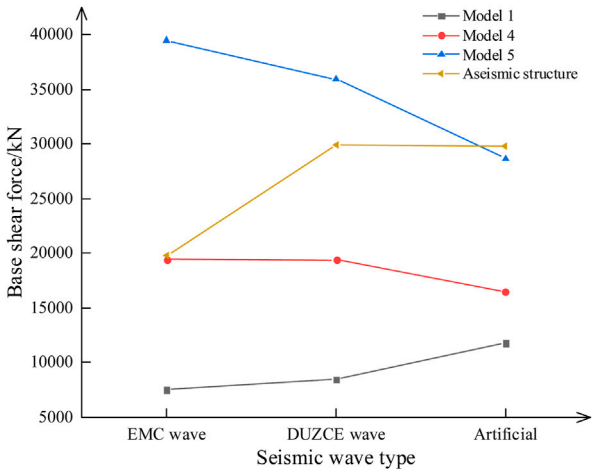

FIGURE 11
The comparison of the base shear force between the aseismic structure and the new staggered story isolated structure with different chassis areas.

different chassis area. According to Table 7, the period of the first three steps of the new staggered story isolated structure is all greater than that of the aseismic structure. And when the position of the upper isolated layer of the new staggered story isolated structure is fixed, the whole modal period of the structure with smaller chassis area is larger.

3.2.2 Basal shear force

Figure 11 depicts the comparison of the base shear force between the aseismic structure and the new staggered story isolated structure with different chassis areas. Figure 11 demonstrates that, compared with the aseismic structure, the base shear force of the new staggered story isolated structure is smaller when the chassis area of the structure is relatively small, and larger when the chassis area of the structure is relatively large. When the position of the upper isolated layer is fixed, the larger the chassis area of the structure, the greater the base shear force and the poorer the isolation effect.

3.2.3 Inter-laminar shear force

The finite element models of the aseismic structure and the new staggered story isolated structure (The upper isolated layer is set at the top of the column of the 3rd floor) are established, whose chassis area is 26 m × 26 m、36 m × 36 m、46 m × 46 m, respectively. The dynamic time history analysis is conducted under the earthquake motions with the seismic fortification intensity of 8° (peak acceleration of 200 cm/s^2). Figure 12 compares the inter-laminar shear force between the aseismic structure and the new staggered story isolated structure; it can be seen that the larger the chassis area of the new staggered story isolated structure is, the greater the shear force on the frame part below the upper isolated layer is, while the shear force on the core tube does not change much. There is little difference in the shear force above the seismic layer of the frame isolated structure. Compared with the seismic structure, the shear force of the new staggered story isolated structure's upper structure is significantly reduced, while the lower frame part is increased.

3.2.4 Story displacement

Figure 13 illustrates the comparison of the story displacement between the aseismic structure and the new staggered story

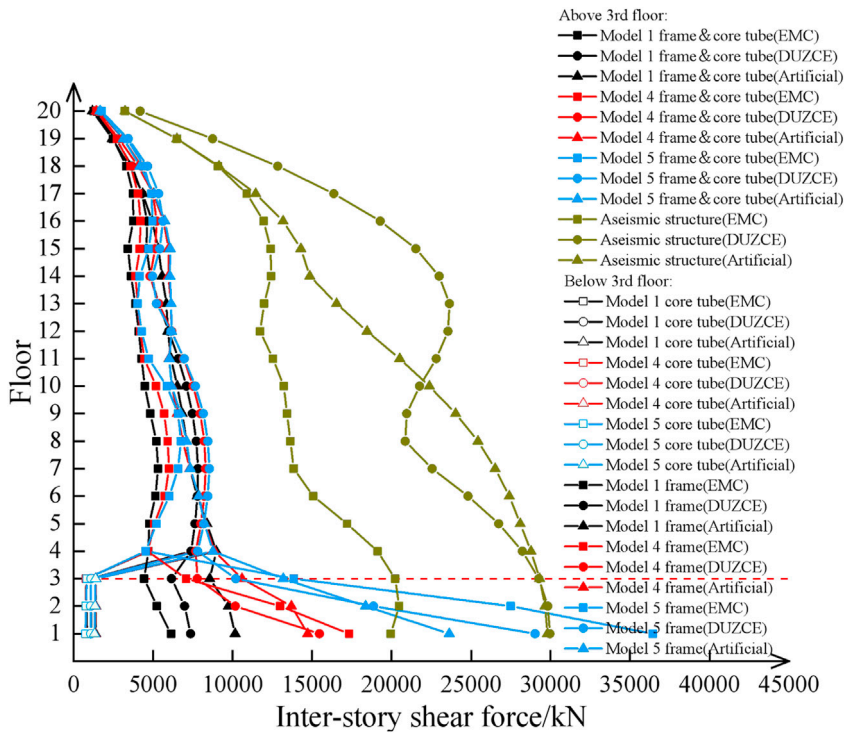

FIGURE 12
Story shear force.

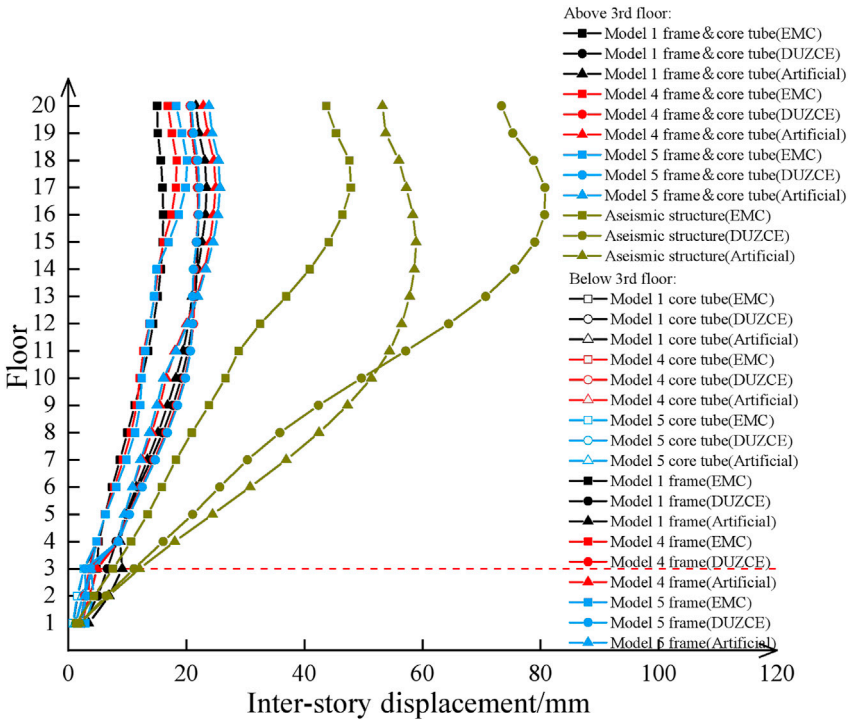

FIGURE 13
Story displacement.

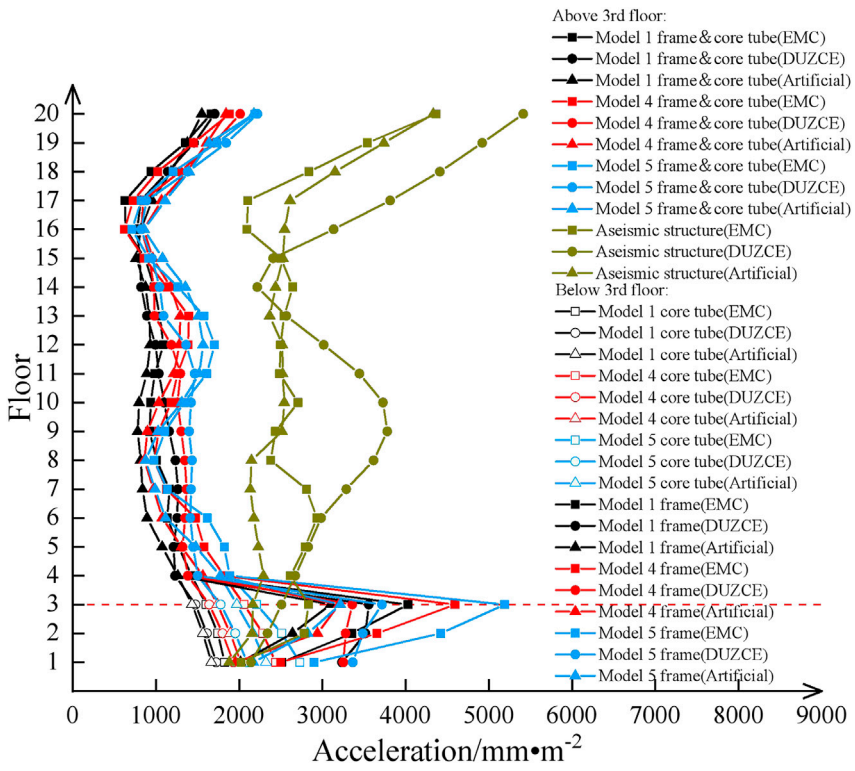

FIGURE 14
Story acceleration.

TABLE 8 Energy consumption of the new staggered story isolated structure.

Type of construction	Earthquake wave	Total seismic input energy (KN·m)	Self damping energy dissipation of structure (KN·m)	Energy consumption of isolated layer (KN·m)	Energy consumption rate of isolated layer (%)	Average decreasing amplitude ratio (%)
Model 1	EMC wave	2018.7762	715.6347	1,287.7836	63.80	70.40
	DUZCE wave	1729.0586	512.2032	1,208.3624	66.90	
	Artificial wave	5,470.6111	1,235.0882	4,234.3644	77.40	
Model 4	EMC wave	2,526.3495	987.3653	1,531.7418	60.60	68.80
	DUZCE wave	1755.1517	510.0222	1,233.7485	70.30	
	Artificial wave	5,879.4096	1,443.8192	4,434.1636	75.40	
Model 5	EMC wave	3,114.0046	1,456.1503	1,650.811	53.00	64.30
	DUZCE wave	1834.5576	566.6311	1,257.2456	68.50	
	Artificial wave	6,314.3731	1811.286	4,501.8078	71.30	

isolated structure (The upper isolated layer is set at the top of the column of the 3rd floor) with the chassis area of 26 m × 26 m、36 m × 36 m、46 m × 46 m respectively. It can be seen from Figure 13 that, compared with the seismic structure, the inter-layer displacement of the new staggered story isolated structure is significantly reduced, and the part above the upper isolated layer is approximately flat. The increase of chassis area has little effect on the story displacement, and the displacement of the frame part below the upper isolated layer is not much different from that of the core tube part.

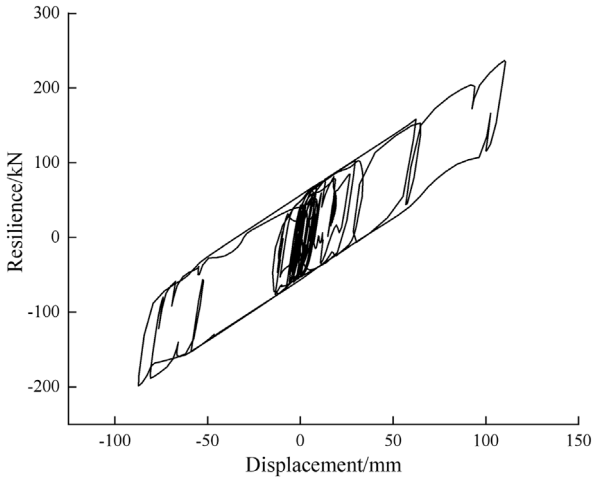

FIGURE 15
Force-displacement hysteresis curve.

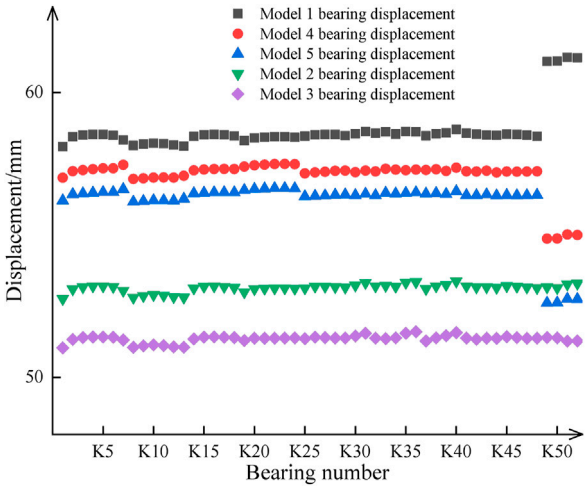

FIGURE 17
Bearing displacement.

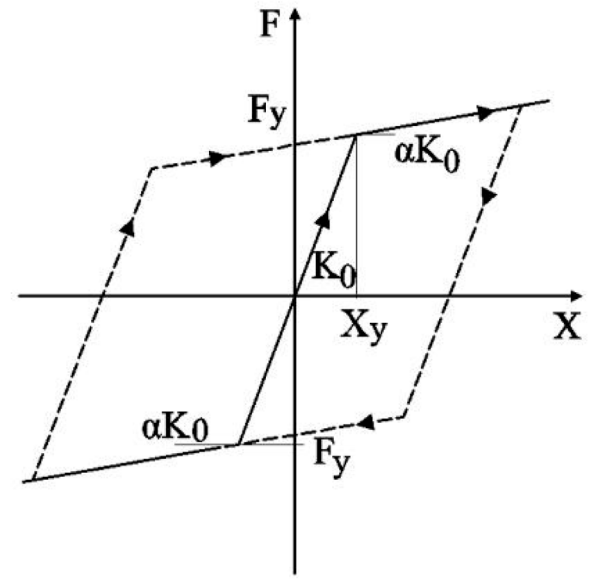

FIGURE 16
Recovery force model of isolation bearing.

3.2.5 Inter-layer acceleration

Figure 14 shows the comparison of the inter-layer acceleration between the aseismic structure and the new staggered story isolated structure (The upper isolated layer is set at the top of the column of the 3rd floor) with the chassis area of 26 m × 26 m、36 m × 36 m、46 m × 46 m respectively. It can be seen that, compared with the seismic structure, the inter-layer acceleration of the new staggered story isolated structure above the upper isolated layer is significantly reduced, and the chassis area below the upper isolated layer increases, which increases the acceleration of the frame part and the core tube part.

3.2.6 Structural energy consumption

The comparison of the energy dissipation between the seismic structure and the new staggered story isolated structure (The upper isolated layer is set at the top of the column of the 3rd floor) with the chassis area of 26 m × 26 m、36 m × 36 m、46 m×46 m respectively is shown in Table 8. It can be seen that when the position of the upper isolated layer of the new staggered story isolated structure remains unchanged, increasing the chassis area is not conducive to the energy consumption of the structure, and the vibration isolated effect of the structure is poor.

4 Response of the isolated bearing

Structural dynamic time history analysis under the peak acceleration of the seismic wave of 400 cm/s^2. Recovery force-displacement hysteresis curve of isolation K 1 under ground motion input is shown in Figure 15. As can be seen from the figure, the hysteretic curve is chaotic under the input of ground motion. In addition to the obvious hysteretic characteristics, it also has certain viscous characteristics, which indicates that the anisotropic responses after the input of ground motion are correlated, so the hysteretic curve of the support is irregular. The restoring force model of isolation bearing is bilinear model, as shown in Figure 16.

4.1 Bearing displacement

Under time-history working conditions, the maximum horizontal displacement of the isolated bearing is equal to the envelope value of the three seismic waves, and this value cannot exceed 0.55 times the effective diameter or 3 times the entire thickness of the rubber bearing according to the standard for building seismic design of GB50011-2010. In this paper, the isolated bearings of LRB600, and LRB1000 are

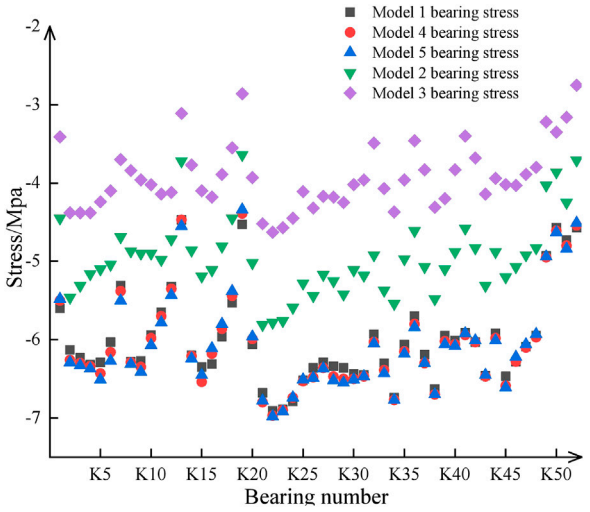

FIGURE 18
Maximum compressive stress of bearing.

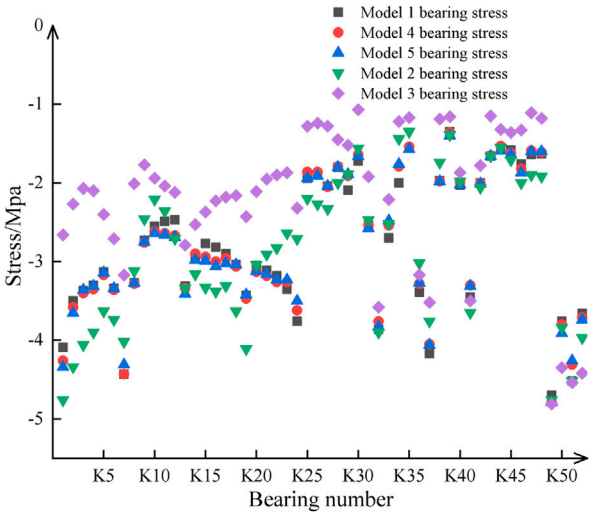

FIGURE 19
Maximum tensile stress of bearing.

employed; hence the minimum bearing displacement is 600× 0.55=330 mm.

After defining the envelope value of the load combination under seismic working conditions and extracting the envelope value of the horizontal displacement of the isolated bearing under time history working conditions of three distinct types of seismic waves, Figure 17 demonstrates that the maximum horizontal displacement of the isolated bearing under the action of the envelope value of the three seismic waves is less than the limit displacement min (0.55d, 3Tr), which meets the standard. Changing the position of the isolated layer and increasing the chassis area of the new staggered story isolated structure have little effect on the displacement of the isolated bearing.

4.2 Stress of isolated bearing

Following the provisions on the maximum tensile stress limit value of the rubber isolated bearing in article 12.2.4 of the code for seismic resistance, the tensile stress of the isolated bearing must not exceed 1 MPa during earthquakes. Generally, 2 times the reference surface pressure can be used as the limit for the maximum surface pressure of the bearing. The structure described in this study is a class B structure, so the reference surface pressure should be 12MPa, and the limit value of the maximum surface pressure is 24 MPa. Since the tensile stiffness of the isolation bearing is only 1/10 of the compressive stiffness, parallel Isolator units and Gap units are used to simulate the isolation bearing.

Figures 18, 19 compare the maximum compressive stress and the maximum tensile stress of the isolated bearing of the new staggered story isolated structure. It can be seen that the maximum compressive stress and the maximum tensile stress of the isolated bearing under the action of the ground motion meet the code requirements, and the bearing located at the core tube is subjected to greater stress.

4.3 Damage research

The comparison of core tube damage and plastic hinge of the new staggered story isolated structure model 1-5 is shown in Figures 20, 21. As can be seen from Figure 18, under the action of ground motion, when the bottom area of the structure is the same, the lower the location of the frame isolation layer is, the less damage will be caused to the core tube of the structure, indicating the better the isolation effect of the structure. When the position of the frame isolation layer of the structure is unchanged, the change of the chassis area of the structure has little influence on the damage of the core tube.

According to Figure 19, under the action of ground motion, when the bottom area of the structure is the same, the position of the isolation layer of the frame is set low, and the fewer plastic hinges appear, indicating that the isolation effect of the structure is better and the safety performance is guaranteed. When the position of the frame isolation layer of the structure remains unchanged, the chassis area of the structure changes. Due to the inconsistent vertical stiffness, plastic hinges appear at the chassis. When the chassis area increases, the upper part of the frame isolation layer also needs to pay attention to the appearance of plastic hinges. The frame column is basically in elasticity, basically meet the LS performance level requirements.

5 Discussion

In this paper, the finite element analysis software ETABS is used to analyze the seismic response of a new staggered story isolated structure. The seismic response analysis and the damage to the seismic structure are investigated from the perspectives of seismic wave, damping effect index, structural damage, energy dissipation, and the response of the isolated bearings. Under the ground motion, it is concluded that the new staggered story isolated structure has a good seismic isolated effect.

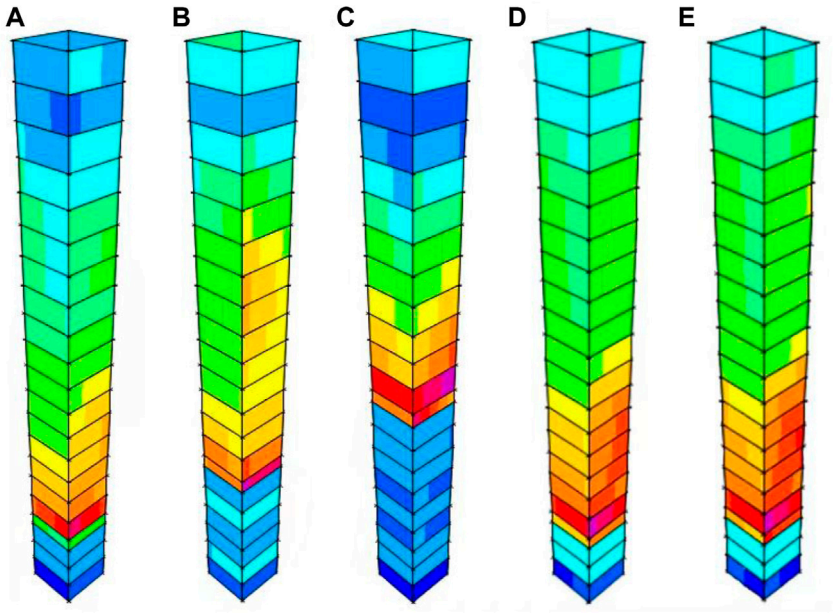

FIGURE 20
Structure diagram:**(A)** Model 1, **(B)** model 2, **(C)** model 3, **(D)** model 4, **(E)** model 5 core tube damage.

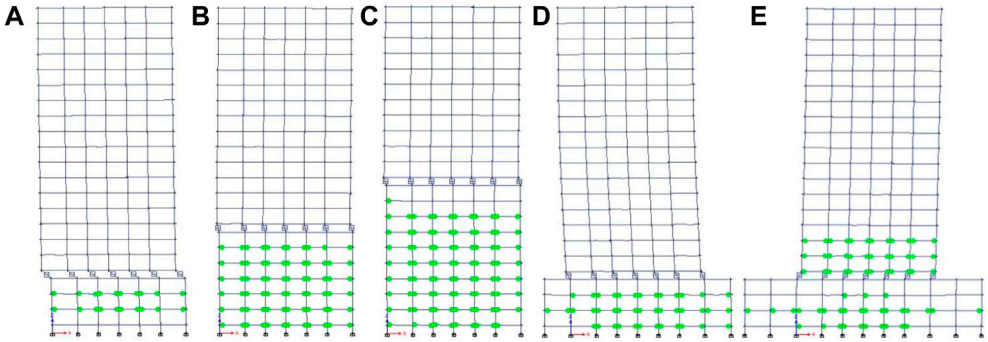

FIGURE 21
Structure diagram:**(A)** Model 1, **(B)** model 2, **(C)** model 3, **(D)** model 4, **(E)** model 5 Plastic hinge.

Further research can be carried out in the following aspects:

1) In this paper, the seismic response analysis of the new staggered layer isolated structure under the ground motion input is mainly based on numerical analysis. Different parameter settings may lead to certain errors in the results (Sugimoto et al., 2016). In the "multi-tower" isolated large chassis structure system, the interaction between the tower and the chassis cannot be ignored. The shaking table tests can be conducted on the new staggered layer isolated structure in the future to verify the analysis presented in this paper.
2) In this paper, the seismic response analysis of the new staggered layer isolated structure is mainly based on the horizontal ground motion (Quaranta et al., 2022; Wang et al., 2022), but the actual earthquakes are multi-dimensional. In many cases, the structure's vertical force under the action of horizontal ground motion is primarily estimated. For some complex structures, the vertical seismic motion must be considered. The isolated effect of different parameters on the structure under vertical earthquakes needs to be further studied.
3) In this paper, the seismic response analysis of a new staggered layer isolated structure under the action of ordinary ground motions is studied. The damage effect differs in different areas under different types of earthquakes. For example, the natural vibration period of the structure is prolonged after being isolated, but the resonance may be generated under the action of a long period of ground motion, which intensifies the seismic response. The seismic response of the new staggered layer isolated structure under different types of ground motion can be studied later.

4) In this paper, the seismic response analysis of the structure is performed with a rigid foundation assumption. In practice, the interaction between the structure and soil presents a challenge and scholars have conducted numerous studies on this issue. The interaction effect of the soil and the structure on the seismic response of an isolated structure is still not clearly studied (Pang, 2013; Askouni and Karabalis, 2022; Zhang and Far, 2022). The negative impact of sandy soils on the dynamic behavior can be solved by optimizing the arrangement of dampers (Aydin et al., 2020). The effect of the interaction between the soil and the structure on the isolated structure of large chassis in new staggered layer isolated structures subjected to ground motions has not yet been investigated.

6 Conclusion

In this paper, the seismic response models of the aseismic structure and the new staggered story isolated structure are developed. Three forms of ground motions are input for the non-linear response analysis, and the discrepancies between the seismic response laws of these two kinds of structures under different ground motions are explored. The following conclusions are obtained:

1) Compared with the seismic structure, the inter-story shear force, inter-story displacement and story acceleration of the new staggered story isolated structure are less, and the new staggered story isolated structure has a greater effect on shock absorption;
2) The lower the isolated layer of the frame of the new staggered layer isolated structure, the better the isolated effect of the structure, the lower the inter-layer shear force, inter-layer acceleration and inter-layer displacement, and the better the energy dissipation effect of the structure, the core tube is less damaged and the plastic hinge is less;
3) By increasing the chassis area of the new staggered layer isolated structure, the part above the frame isolated layer will have a good isolated effect, while the shear force and acceleration of the part below the frame isolated layer increase instead, the damage at the core tube changed little and the appearance of plastic hinge increased;
4) Under rare earthquakes, when the position of the frame isolated layer and the area of the chassis of the new staggered layer isolated structure change, the displacement, tensile stress and compressive stress of the isolated bearing all meet the specification requirements.

Data availability statement

The raw data supporting the conclusions of this article will be made available by the authors, without undue reservation.

Author contributions

TS, DL, and SY contributed to conception and design of the study. TS wrote the first draft of the manuscript. All authors contributed to manuscript revision, read, and approved the submitted version.

Conflict of interest

The authors declare that the research was conducted in the absence of any commercial or financial relationships that could be construed as a potential conflict of interest.

Publisher's note

Supplementary material

The Supplementary Material for this article can be found online at: https://www.frontiersin.org/articles/10.3389/feart.2023.1115235/full#supplementary-material

References

Askouni, P., and Karabalis, D. (2022). The modification of the estimated seismic behaviour of r/c low-rise buildings due to ssi. *Buildings* 12, 975. doi:10.3390/buildings12070975

Aydin, E., Ozturk, B., Bogdanovic, A., and Farsangi, E. N. (2020). "Influence of soil-structure interaction (SSI) on optimal design of passive damping devices," in *Structures* (Elsevier), 28, 847–862.

Cancellara, D., and De Angelis, F. (2016). Nonlinear dynamic analysis for multi-storey rc structures with hybrid base isolation systems in presence of bi-directional ground motions. *Compos Struct.* 154, 464–492. doi:10.1016/j.compstruct.2016.07.030

Chang, Z., Catani, F., Huang, F., Liu, G., Meena, S. R., Huang, J., et al. (2022a). Landslide susceptibility prediction using slope unit-based machine learning models considering the heterogeneity of conditioning factors. *J. Rock Mech. Geotechnical Eng.* doi:10.1016/j.jrmge.2022.07.009

Chang, Z., Du, Z., Zhang, F., Huang, F., Chen, J., Li, W., et al. (2022b). Landslide susceptibility prediction based on remote sensing images and gis: Comparisons of supervised and unsupervised machine learning models. *Remote Sens.* 12, 502. doi:10.3390/rs12030502

Donà, M., Bernardi, E., Zonta, A., Tan, P., and Zhou, F. (2021). Evaluation of optimal FVDs for inter-storey isolation systems based on surrogate performance models. *Bull. Earthquake Eng.* 19 (11), 4587–4621.

Erdik, M., Ulker, O., Sadan, B., and Tuzun, C. (2018). Seismic isolation code developments and significant applications in Turkey. *Soil Dyn. Earthq. Eng.* 115, 413–437. doi:10.1016/j.soildyn.2018.09.009

Faiella, D., Calderoni, B., and Mele, E. (2020). Seismic retrofit of existing masonry buildings through inter-story isolation system: A case study and general design criteria. *J. Earthq. Engeer* 26, 2051–2087. doi:10.1080/13632469.2020.1752854

Fujii, K. (2022). *Influence of the angle of seismic incidence of long-period pulse-like ground motion on an irregular base-isolated building.*

Guo, Z. Z., Shi, Y., Huang, F. M., Fan, X. M., and Huang, J. S. (2021). Landslide susceptibility zonation method based on c5.0 decision tree and k-means cluster

algorithms to improve the efficiency of risk management. *Geosci. Front.* 12, 101249. doi:10.1016/j.gsf.2021.101249

Hayashi, K., Fujita, K., Tsuji, M., and Takewaki, I. (2018). A simple response evaluation method for base-isolation building-connection hybrid structural system under long-period and long-duration ground motion. *Front. Built Environ.* 4. doi:10.3389/fbuil.2018.00002

Hessabi, R. M., Mercan, O., and Ozturk, B. (2017). Exploring the effects of tuned mass dampers on the seismic performance of structures with nonlinear base isolation systems. *Earthquakes Struct.* 12 (3), 285–296. doi:10.12989/eas.2017.12.3.285

Huang, F., Cao, Z., Guo, J., Jiang, S-H., Li, S., and Guo, Z. (2020a). Comparisons of heuristic, general statistical and machine learning models for landslide susceptibility prediction and mapping. *CATENA* 191, 104580. doi:10.1016/j.catena.2020.104580

Huang, F., Cao, Z., Jiang, S-H., Zhou, C., Huang, J., and Guo, Z. (2020b). Landslide susceptibility prediction based on a semi-supervised multiple-layer perceptron model. *Landslides* 17.

Huang, F., Chen, J., Liu, W., Huang, J., Hong, H., and Chen, W. (2022c). Regional rainfall-induced landslide hazard warning based on landslide susceptibility mapping and a critical rainfall threshold. *Geomorphology* 408, 108236. doi:10.1016/j.geomorph.2022.108236

Huang, F., Zhang, J., Zhou, C., Wang, Y., Huang, J., and Zhu, L. (2020d). A deep learning algorithm using a fully connected sparse autoencoder neural network for landslide susceptibility prediction. *Landslides* 17, 217–229. doi:10.1007/s10346-019-01274-9

Hur, M. W., and Park, T. W. (2022). Seismic performance of story-added type buildings remodeled with story seismic isolation systems. *Buildings* 12, 270. doi:10.3390/buildings12030270

Jiang, S-H., Huang, J., Huang, F., Yang, J., Yao, C., and Zhou, C. (2018). Modelling of spatial variability of soil undrained shear strength by conditional random fields for slope reliability analysis. *Appl. Math. Model.* 63, 374–389. doi:10.1016/j.apm.2018.06.030

Köroğlu, A. (2022). *Rehabilitation of building structures with soft story irregularity via optimal viscous damper distribution.*

Li, F., Wang, L., and Wu, Y. (2021). Seismic response reduction analysis of large chassis base-isolated structure under long-period ground motions. *Earthq. Res. Adv.* 1 (2), 100026. doi:10.1016/j.eqrea.2021.100026

Li, W., Wang, S., Miao, Q., and Liu, J. (2014). Nonlinear stimulation of reinforced masonry structure and adding-story isolation model. *China Civ. Engeerning J.* 47, 35–40.

Li, Z. H., Huang, G. Q., Chen, X. Z., and Zhou, X. H. (2022). Seismic response and parametric analysis of inter-story isolated tall buildings based on enhanced simplified dynamic model. *Int. J. Struct. Stab. Dyn.* 22, 2240008. doi:10.1142/s0219455422400089

Liu, D. W., Li, L. P., Zhang, Y. F., Chen, L. H., Wan, F., and Yang, F. (2022). Study on seismic response of a new staggered story isolated structure considering ssi effect. *J. Civ. Eng. Manag.* 28, 397–407. doi:10.3846/jcem.2022.16825

Losanno, D., Ravichandran, N., Parisi, F., Calabrese, A., and Serino, G. (2021). Seismic performance of a low-cost base isolation system for unreinforced brick masonry buildings in developing countries. *Soil Dyn. Earthq. Eng.* 141, 106501. doi:10.1016/j.soildyn.2020.106501

Ma, X. T., Bao, C., Shu Ing, D., Lu, H., Zhang, L. X., Ma, Z. W., et al. (2020). Dynamic response analysis of story-adding structure with isolation technique subjected to near-fault pulse-like ground motions. *Phys. Chem. Earth, Parts A/B/C* 121, 102957. doi:10.1016/j.pce.2020.102957

Micozzi, F., Flora, A., Viggiani, L. R. S., Cardone, D., Ragni, L., and Dall'Asta, A. (2022). Risk assessment of reinforced concrete buildings with rubber isolation systems designed by the Italian seismic code. *J. Earthq. Eng.* 26 (14), 7245–7275. doi:10.1080/13632469.2021.1961937

Nobari Azar, F. A., Karimzadeh Naghshineh, A., and Sen, M. (2022). *Preparation and characterization of natural rubber–based new elastomers for high-damping base isolation systems.* Journal of Elastomers & Plastics, 00952443221075505.

Ozturk, B., Cetin, H., Dutkiewicz, M., Aydin, E., and Noroozinejad Farsangi, E. (2022). On the efficacy of a novel optimized tuned mass damper for minimizing dynamic responses of cantilever beams. *Appl. Sci.* 12 (15), 7878. doi:10.3390/app12157878

Pang, Y. B. (2013). "Seismic response analysis of soil-structure interaction on base isolation structure," in *Advanced materials research* (Trans Tech Publications Ltd), 663, 87–91.

Pang, Y. B. (2012). "Seismic response analysis on two-tower isolated structure with enlarged base," in *Applied mechanics and materials* (Trans Tech Publications Ltd), 193, 753–756.

Park, W., and Ok, S. Y. (2021). Hybrid optimization design approach of asymmetric base-isolation coupling system for twin buildings. *J. Low Freq. Noise Vib. Act. Control* 40, 1993–2013. doi:10.1177/1461348421992969

Pérez-Rocha, L. E., Avilés-López, J., and Tena-Colunga, A. (2021). Base isolation for mid-rise buildings in presence of soil-structure interaction. *Soil Dyn. Earthq. Eng.* 151, 106980. doi:10.1016/j.soildyn.2021.106980

Qahir Darwish, A., and Bhandari, M. (2022). Seismic response reduction of high rise steel-concrete composite buildings equipped with base isolation system. *Mater Today Proc.* 59, 516–524. doi:10.1016/j.matpr.2021.11.560

Quaranta, G., Angelucci, G., and Mollaioli, F. (2022). Near-fault earthquakes with pulse-like horizontal and vertical seismic ground motion components: Analysis and effects on elastomeric bearings. *Soil Dyn. Earthq. Eng.* 160, 107361. doi:10.1016/j.soildyn.2022.107361

Rabiee, R., and Chae, Y. (2022). Real-time hybrid simulation for a base-isolated building with the transmissibility-based semi-active controller. *J. Intelligent Material Syst. Struct.* 33, 2228–2240. doi:10.1177/1045389x221079680

Saha, A., and Mishra, S. K. (2021a). Implications of inter-storey-isolation (isi) on seismic fragility, loss and resilience of buildings subjected to near fault ground motions. *Bull. Earthq. Eng.* 20, 899–939. doi:10.1007/s10518-021-01277-9

Saha, A., and Mishra, S. K. (2021b). Amplification of seismic demands in inter-storey-isolated buildings subjected to near fault pulse type ground motions. *Soil Dyn. Earthq. Eng.* 147, 106771. doi:10.1016/j.soildyn.2021.106771

Sugimoto, K., Yonezawa, K., Katsumata, H., and Fukuyama, H. (2016). Shaking table test of quarter scale 20 story rc moment frame building subjected to long period ground motions. *J. Disaster Res.* 11, 97–105. doi:10.20965/jdr.2016.p0097

Vibhute, A. S., Bharti, S. D., Shrimali, M. K., and Datta, T. K. (2022). "Performance evaluation of FPS and LRB isolated frames under main and aftershocks of an earthquake," in *Structures* (Elsevier), 44, 1532–1545.

Wang, L., and Lei, H. (2021). Structural analysis of a multi-tower building with a large chassis in a business district IOP conference series: Earth and environmental science. *IOP Publ.* 647 (1), 012175. doi:10.1088/1755-1315/647/1/012175

Wang, L., Nagarajaiah, S., Shi, W., and Zhou, Y. (2022). Seismic performance improvement of base-isolated structures using a semi-active tuned mass damper. *Eng. Struct.* 271, 114963. doi:10.1016/j.engstruct.2022.114963

Wu, Y., Lu, J., and Qi, A. (2019). Shaking table test and numerical analysis of mid-story isolation eccentric structure with tower–podium. *Adv. Mech. Eng.* 11 (1), 168781401881956. doi:10.1177/1687814018819562

Zhang, H., Li, F., Tai, J., and Zhou, J. (2021). Research on structural design of an isolated high-rise building with enlarged base and multiple tower layer in high-intensity area. *Math. Problems Eng.* 2021, 1–14. doi:10.1155/2021/6669388

Zhang, S., Hu, Y., Zhang, C., Li, S., and Tan, P. (2022). Performance-based compositive passive control analysis of multi-tower building with chassis: Optimization of kelvin-voigt dampers. *Buildings* 12 (2), 137. doi:10.3390/buildings12020137

Zhang, X., and Far, H. (2022). Effects of dynamic soil-structure interaction on seismic behaviour of high-rise buildings. *Bull. Earthq. Eng.* 20, 3443–3467. doi:10.1007/s10518-021-01176-z

Zhang, Y. F., Liu, D. W., Fang, S. T., Lei, M., Zhu, Z. H., and Liao, W. Y. (2022). Study on shock absorption performance and damage of a new staggered story isolated system. *Adv. Struct. Eng.* 25, 1136–1147. doi:10.1177/13694332211056113

Zhao, D., Wang, H., Qian, H., and Liu, J. (2022). Comparative vulnerability analysis of decomposed signal for the LRB base-isolated structure under pulse-like ground motions. *J. Build. Eng.* 59, 105106. doi:10.1016/j.jobe.2022.105106

Zhou, Y., Chen, P., Wang, C., Zhang, L., and Lu, L. (2018). Seismic performance evaluation of tall, multitower reinforced concrete buildings with large bottom podiums. *Struct. Concr.* 19 (6), 1591–1607. doi:10.1002/suco.201700142